The background of the slide is a light blue gradient with several realistic water droplets of various sizes scattered across it. The droplets have highlights and shadows, giving them a three-dimensional appearance.

**BREAKTHROUGH IN CORRUGATED
CONICAL HORN RESEARCH IN QUEEN
MARY COLLEGE. UNIVERSITY OF LONDON
DURING LATE 1960'S**

A REMINISCENCE BY PRADIP KUMAR SAHA

Search for Low-Noise Feed Horns: Situation in 1960s

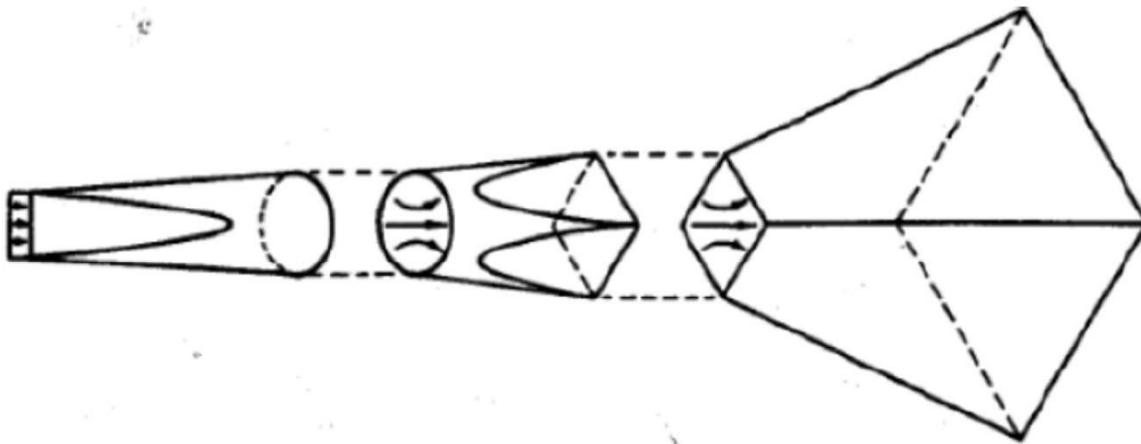
Desired Characteristics:

- ❖ **High Efficiency**
- ❖ **Co-polar Pattern Symmetry**
- ❖ **Low (-30 dB or better) sidelobes**

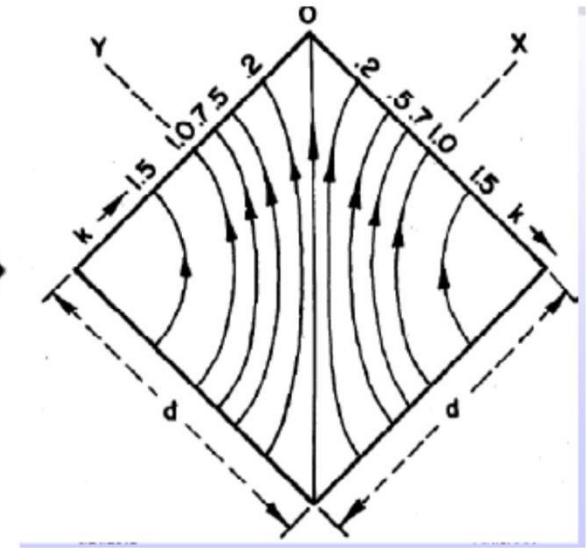
Among various structures invented, perhaps the most notable, most ingenious were:

- (1) Diagonal Horn (1962)–a shaped-aperture horn**
- (2) Potter Horn (1963)–a dual-mode conical horn.**

Diagonal Horn



Rectangular waveguide to diagonally polarized horn – Mode transducer

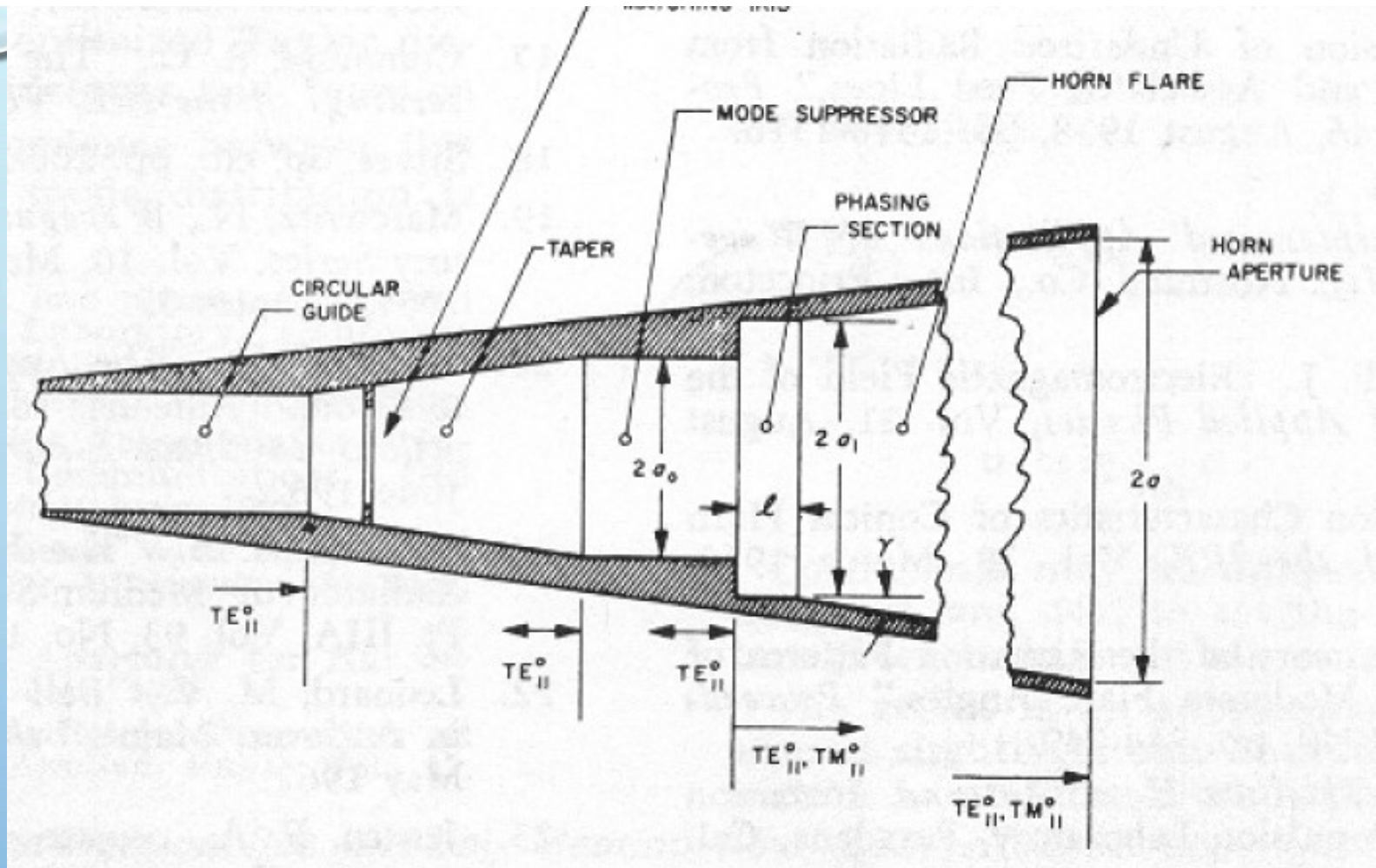


The field pattern in the aperture

Diagonal Horn

It is a small-flare shaped-aperture (square-aperture) pure-mode horn that is diagonally polarized.

- ❖ The co-polar pattern is almost circularly symmetric, but**
- ❖ the peak cross-polar level is as high as -16 dB in the $\pm 45^\circ$ planes.**
- ❖ The sidelobes in the principal planes are about -20 dB.**



Dual-mode Potter Horn

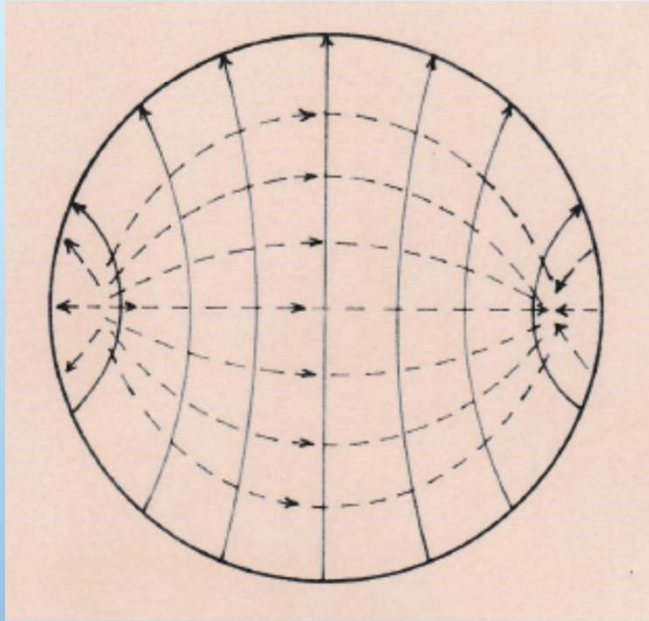
Potter Horn

Potter horn used both circular TE_{11} and TM_{11} modes in proper amplitude ratio to achieve

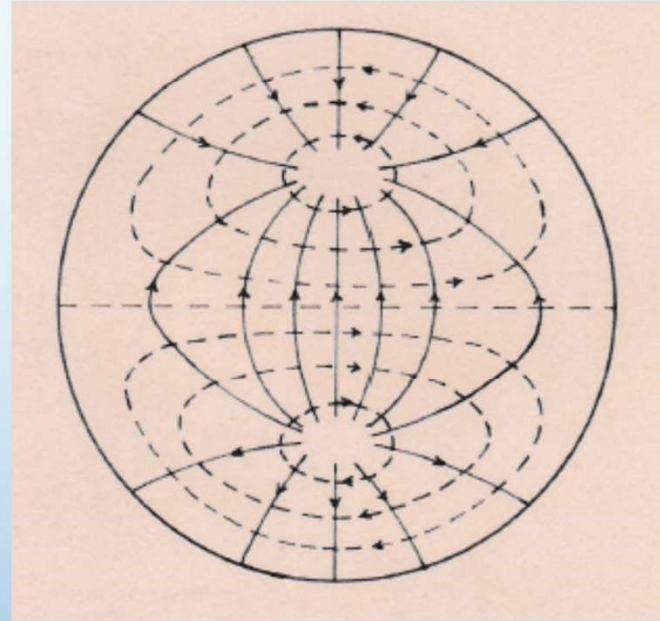
- ❖ aperture distribution tapered to zero in all planes,
- ❖ complete beam-width equalization in all planes,
- ❖ complete phase-centre coincidence in all planes,
- ❖ at least -30 dB sidelobe level in E-plane.
- ❖ H-plane performance remains unchanged.

Disadvantages:

- ❖ Narrowband
- ❖ Since TM_{11} does not radiate axially, Potter horn has lower gain than a TE_{11} horn of same aperture size.
- ❖ Elaborate design procedure.



TE₁₁



TM₁₁

Wide-Flare Conical Horn: A. F. Kay (1962)

- ❖ Such horns are characterized by Δ (the maximum phase deviation of spherical phase front from aperture plane) $> \lambda/2$, unlike “diffraction limited” horns with $\Delta < \lambda/2$.
- ❖ Phase centres are at the throat of the horn.
- ❖ Patterns have virtually no sidelobes.
- ❖ Beamwidth, to first approximation, is independent of λ .
- ❖ At $\theta = \theta_0$ (Half Flare Angle), E-plane pattern level is 6-9 dB depending on θ_0 and independent of λ ; in H-plane it is 13-25 dB depending on θ_0 and slightly on Flare Length/ λ ratio.
- ❖ Heavy E-plane edge illumination spoils phase-centre coincidence and lowers secondary aperture efficiency.

Phase Centre Location in Feedhorn

When a feed with widely separated E-plane and H-plane phase centres illuminates a reflector, there is inevitable axial de-focusing. This -

- **reduces the antenna gain,**
- **raises the side-lobe level in a symmetrical way,**
- **and, most importantly in some applications, raises the peak level of cross-polarization in the 45° plane.**

Wide-Flare Corrugated Conical Horn: A. F. Kay (1964)

- ❖ **If the inner wall of wide-flare conical horn was corrugated with transverse grooves that present capacitive series reactance to the incident field in the E-plane, radiation patterns are almost symmetrical over a broad frequency band.**
- ❖ **This indicated that the boundary conditions for the radially flowing field are the same in every axial plane independent of polarization.**
- ❖ **This was explained from an analogy with plane corrugated surface.**

- ❖ If a plane wave, traveling transverse to the grooves on a plane corrugated surface, is incident at an angle ψ to the perpendicular to the surface, the reflection coefficients for TE/TM waves are given by

$$R_{TE} = -1$$

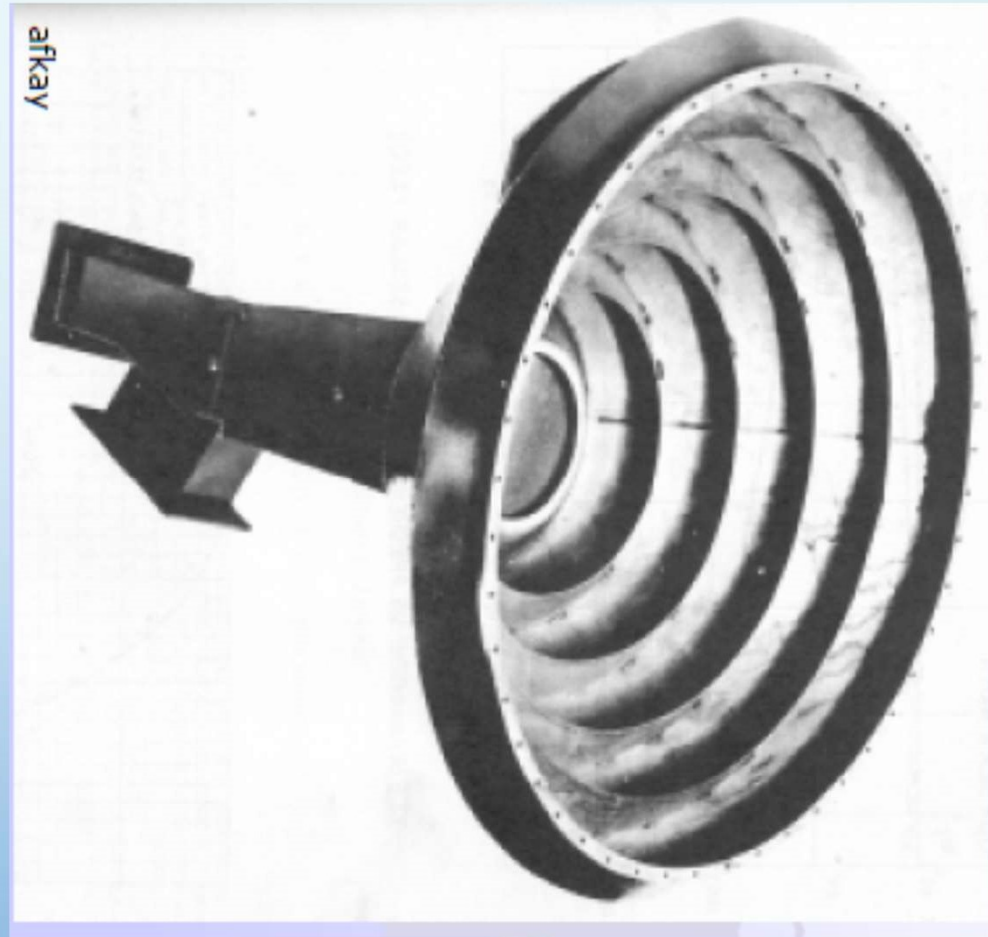
$$R_{TM} = \frac{\cos \psi + jX}{\cos \psi - jX}$$

where X is the surface reactance.

- ❖ In the limit $\psi \rightarrow 90^\circ$, $R_{TE} = R_{TM} \rightarrow -1$. Implication: on the corrugated surface, tangential components of both E and H vanish.
- ❖ This can be true for both inductive ($X > 0$) and capacitive ($X < 0$) surfaces.
- ❖ Inductive surface is inappropriate for antenna applications as it supports surface waves which do not vanish on the surface. Only capacitive surface is desirable.
- ❖ Thus, a boundary condition which is independent of polarization, produces a field that is independent of polarization. Accordingly, such a feed was named – **SCALAR FEED.**

Scalar Feed
Half Flare Angle - 70°

A. F. Kay (1964)



Hybrid Mode Waveguide Feed: Minnett and Thomas (1966)

- ❖ **Study of the focal field of a circularly symmetric parabolic reflector, illuminated by a linearly polarized plane wave, together with the concept of symmetric radiation field led to the development of hybrid mode waveguide feeds.**
- ❖ **The scattered field at the focal plane of the reflector is a superposition of axially propagating hybrid waves that were identified with the fast hybrid modes of unit azimuthal dependence in a transversely corrugated circular waveguide.**

- ❖ It was shown that a waveguide to support the focal-field hybrid waves, its boundary must satisfy $X_z \cdot X_\xi = -\eta_0^2$, where X_z is longitudinal surface reactance and X_ξ is circumferential surface reactance, η_0 is free-space wave impedance.
- ❖ Transversely corrugated surface with appropriate groove depth and sufficient number of corrugations per wavelength, approximately satisfies this condition with $X_z = \infty$ and $X_\xi = 0$.
- ❖ The condition can also be satisfied by longitudinally grooved surface with $X_z = 0$ and $X_\xi = \infty$. However, with such boundary, the waveguide would support pure TM_{1n} modes and hence would be unsuitable.

**In this backdrop,
P.J.B.Clarricoats and his research student
Pradip Kumar Saha entered the fray in 1968.**

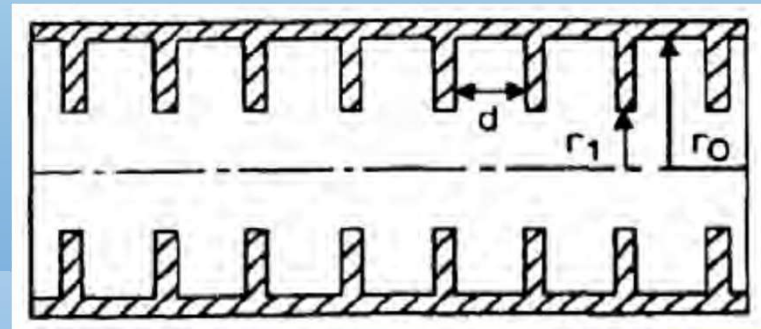
**Aim: Study of Propagation and Radiation
Characteristics of Fast Waves in Corrugated
Circular Waveguides and Corrugated
Conical Horns**

Study of Fast Wave Propagation in Transversely Corrugated Circular Waveguide

- Characteristic Equation
- Circularly Symmetric Modes
- Azimuthally Dependent Hybrid Modes
- Dispersion Diagrams
- Balanced Hybrid Condition

Lowest Hybrid Mode HE_{11}

- Field Pattern
- Power Flow
- *Attenuation*



Slot Depth $g=r_0-r_1$,
Slot Width= d

Balanced Hybrid Condition

Perfect pattern symmetry and zero cross-polarization occur at the design frequency under “**Balanced Hybrid**” condition (BHC), when the corrugation depth is about one quarter of the wavelength.

For large apertures (large waveguide radii), slot depth g (for BHC) $\approx \lambda/4$. For small apertures $g > 0.25\lambda$, being $\approx 0.3\lambda$ for 2λ aperture.

Example: For a 10 GHz horn with aperture diameter of 3λ , slot depth of 0.3λ , peak cross-polar level in 45° plane is -47 dB.

Dimensionless Hybrid Factor $\bar{\Lambda}$

$$\bar{\Lambda} = j\eta_0 \frac{H_z}{E_z} = -m \frac{(\beta_{mn}/k_0)}{F_m(k_{cmn}/r_1)}$$

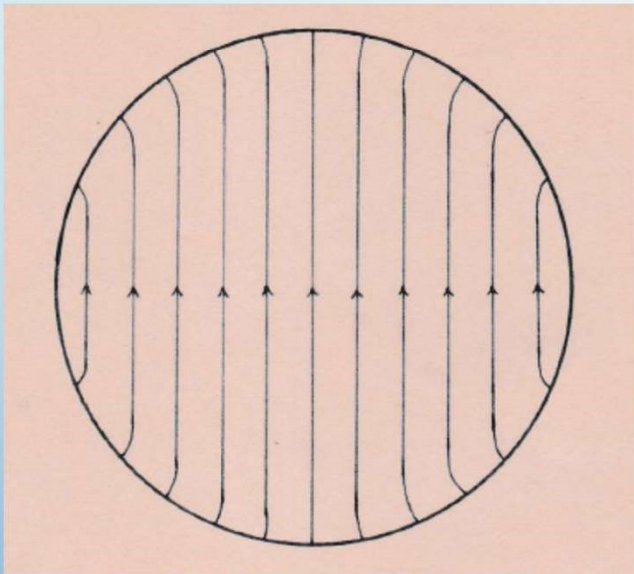
$$F_m(x) = x \frac{J'_m(x)}{J_m(x)}$$

$\bar{\Lambda} = 0$ for TM modes ; $1/\bar{\Lambda} = 0$ for TE modes
= ± 1 for hybrid modes under BHC

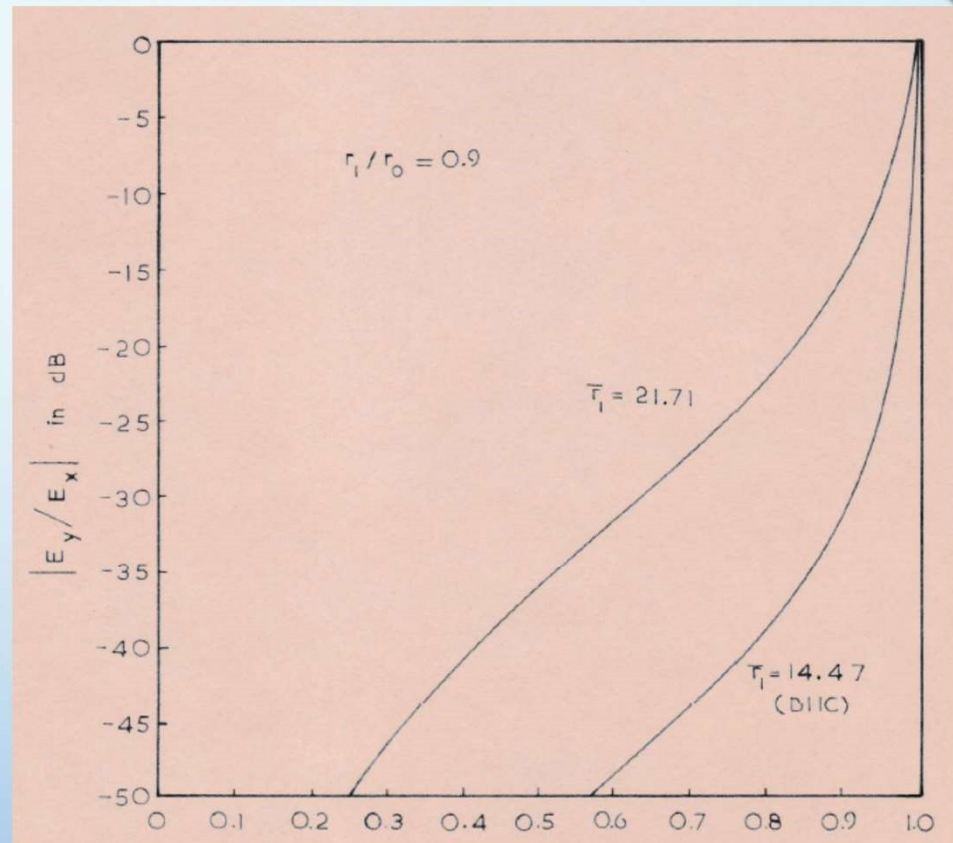
Upper sign for HE_{mn} modes

Lower sign for EH_{mn} modes

Fields in Corrugated Waveguide



Transverse E Field
of Balanced HE_{11} Mode



r/r_1
Cross-polar Component of HE_{11} Mode
in 45° Plane

Attenuation in Corrugated Circular Waveguide

The Theoretical attenuation of HE_{11} mode under balanced hybrid condition and over a band around the frequency corresponding to BHC can be lower than the attenuation in a TE_{11} circular waveguide of same diameter $2r_1$.



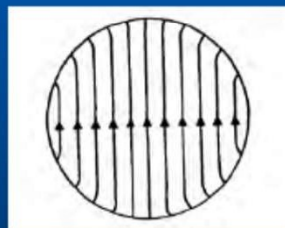
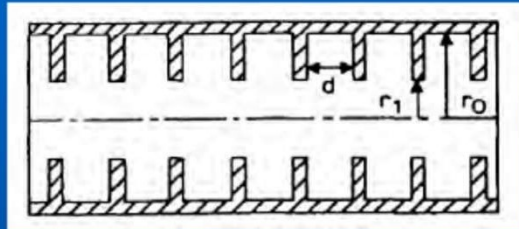
Transmission of Light in Fiber for Optical Communication

Mrs. Gwen MW Kao
on behalf of
Professor Charles K Kao
Nobel Laureate in Physics 2009

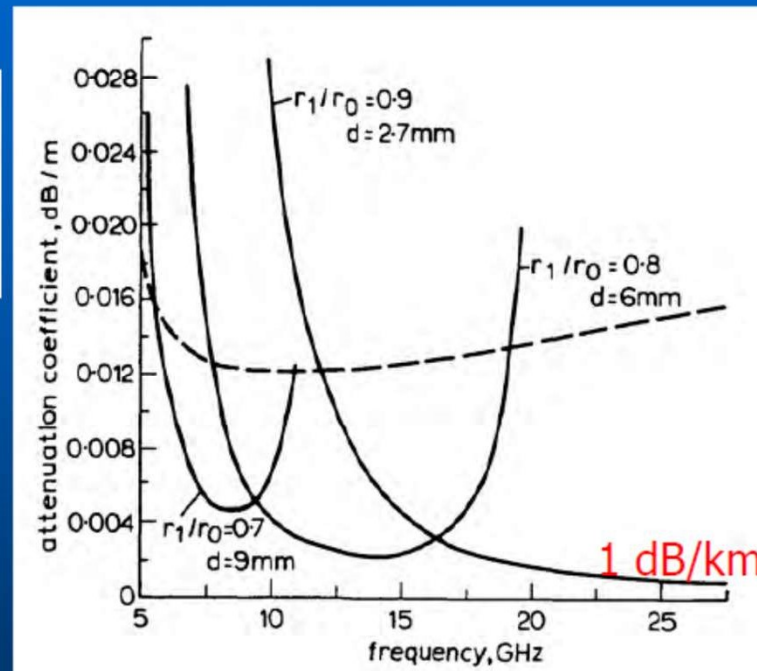
8 December 2009
Aula Magna
Stockholm University

The Chinese University of Hong Kong

Low-loss corrugated circular waveguide



HE11 Mode

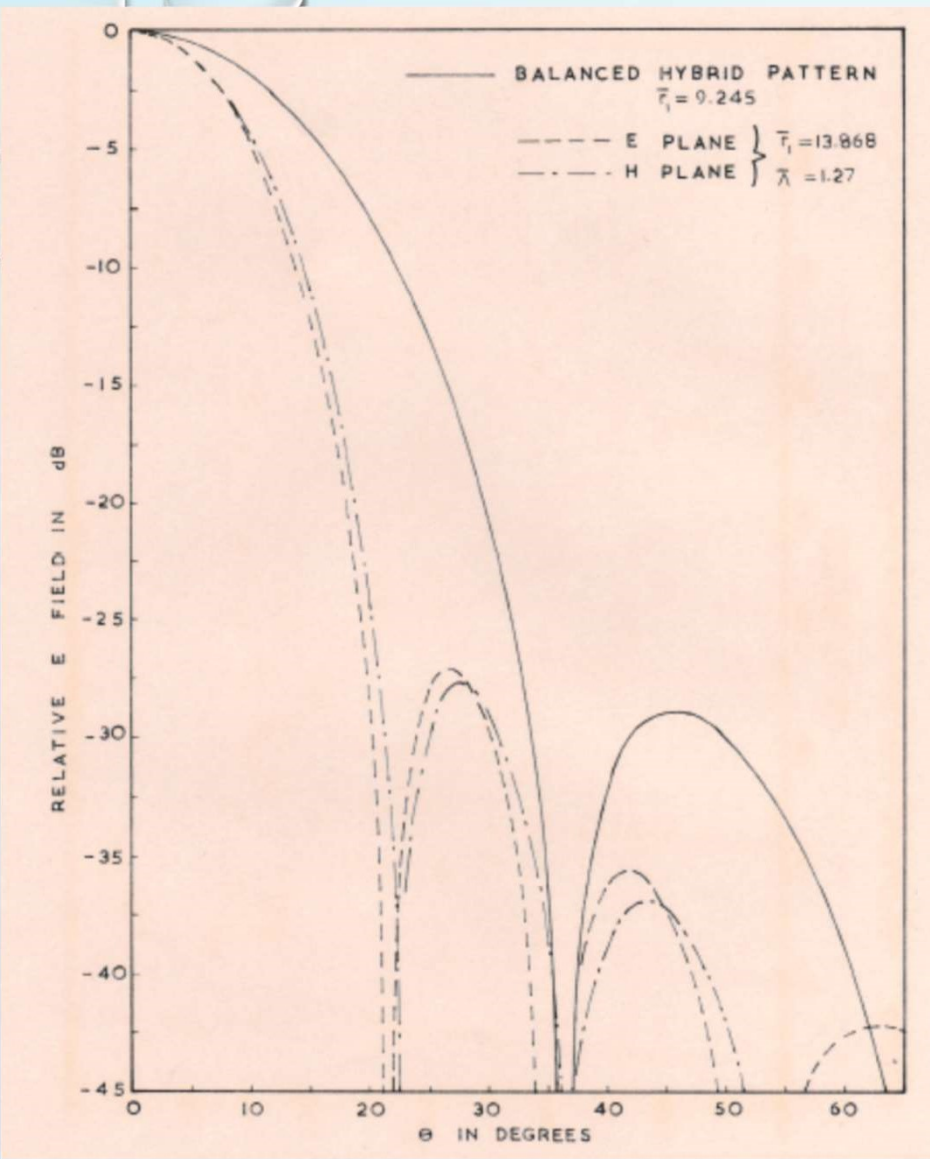


P.J.B. Clarricoat & P.K. Saha, "Attenuation in Corrugated Circular Waveguide," *Elect. Lett.*, Vol. **12**, pp.370-2, 1970.

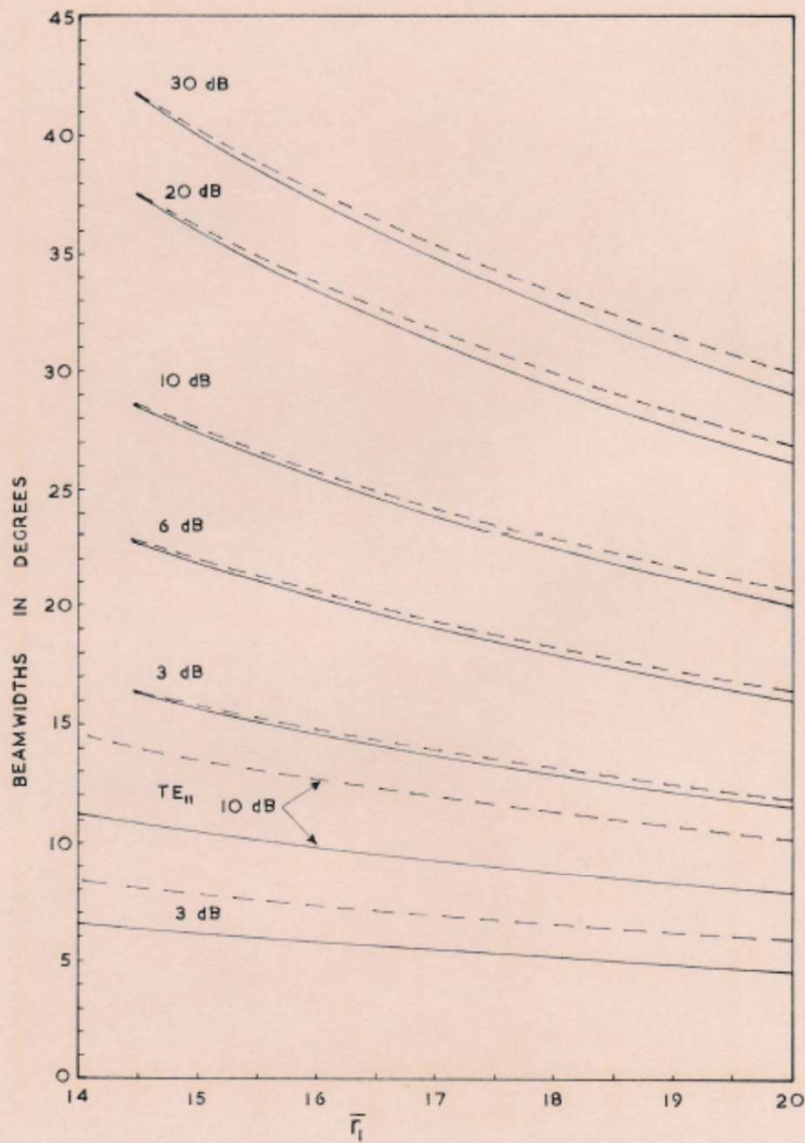


Radiation From Corrugated Circular Waveguide

- **Far-field Pattern by Kirchhoff-Huygen Integration**
- **Hybrid Mode Radiation Fields**
- **HE₁₁ Mode Radiation Patterns**
- **Performance of Parabolic Reflector with Corrugated Waveguide Feed**
- **An Experimental Narrow-Flare (12° half flare) Corrugated Horn**
- **Measured Patterns and Input VSWR: 8.5 – 11.0 GHz**

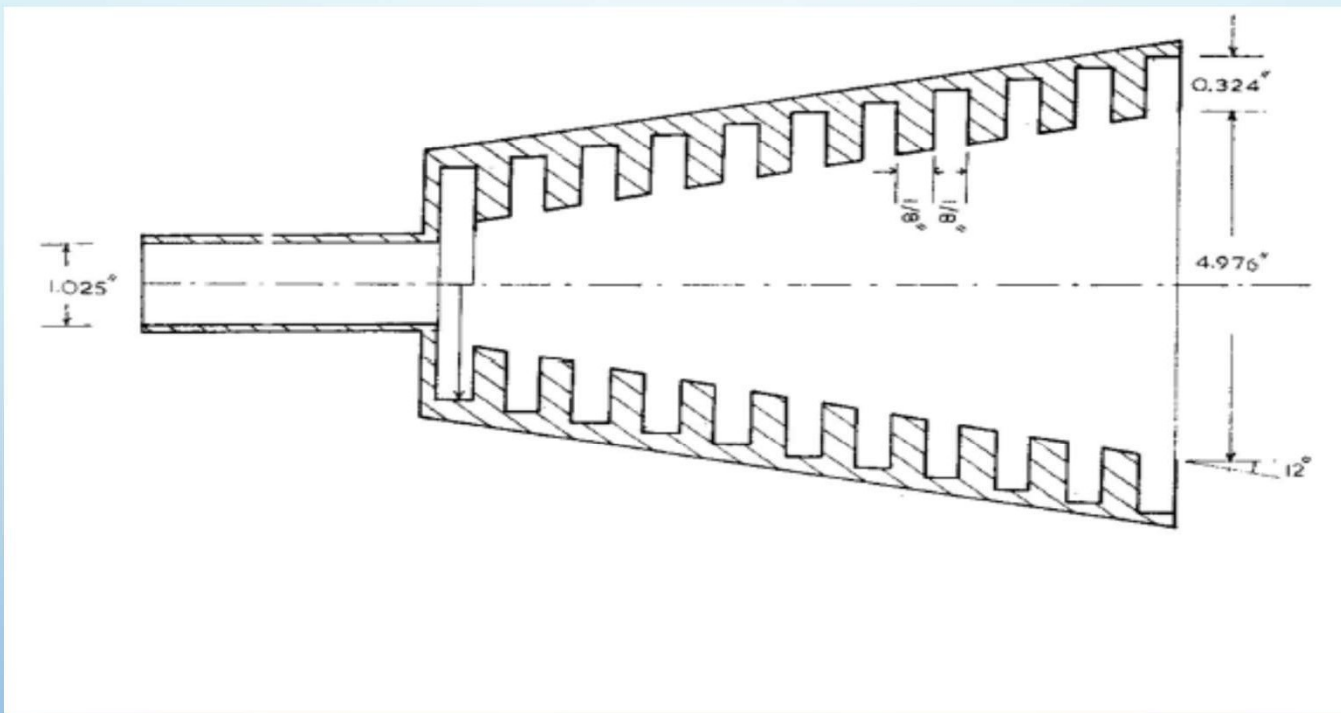


Theoretical Radiation Patterns of HE₁₁ Mode in Corrugated Circular Waveguide under BHC and at 1.5 times higher frequency



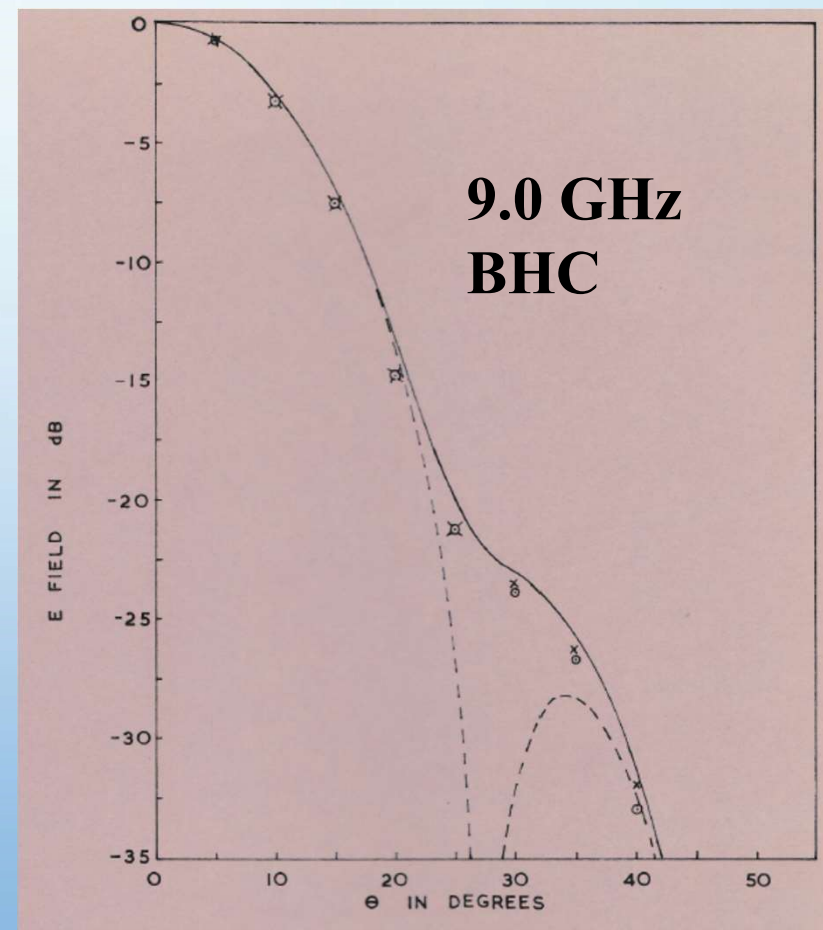
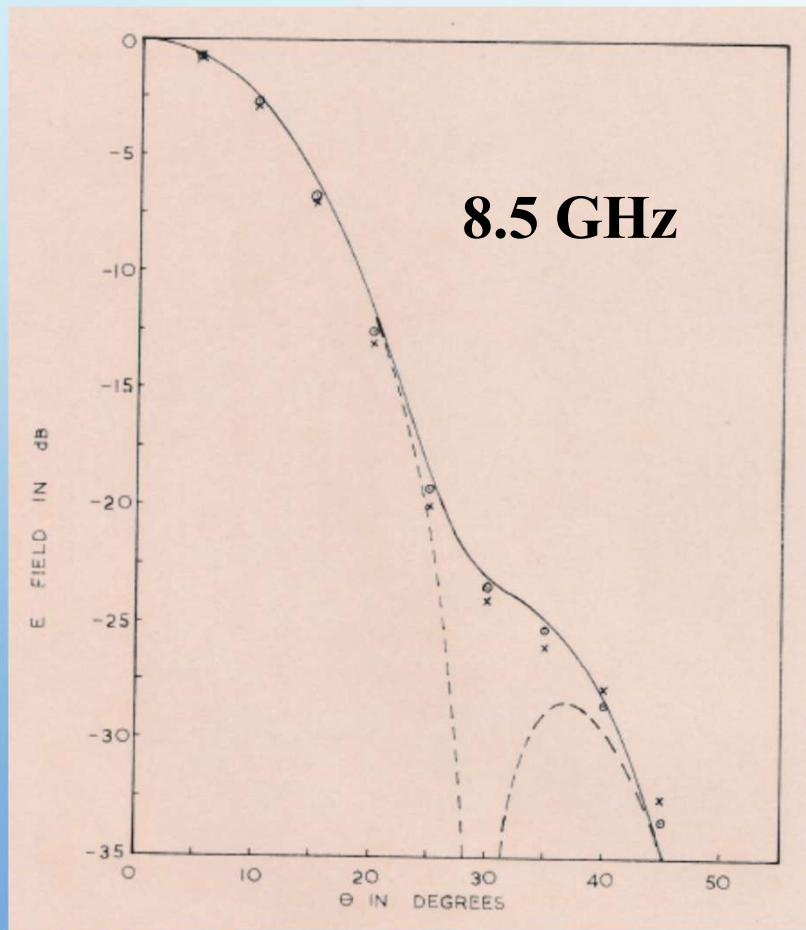
**E-plane (—), H-plane (- - -)
 Beamwidths of HE_{11} Radiation
 Pattern of Corrugated Circular
 Waveguide as function of
 Normalized Frequency
 ($r_1/r_0 = 0.9$)**

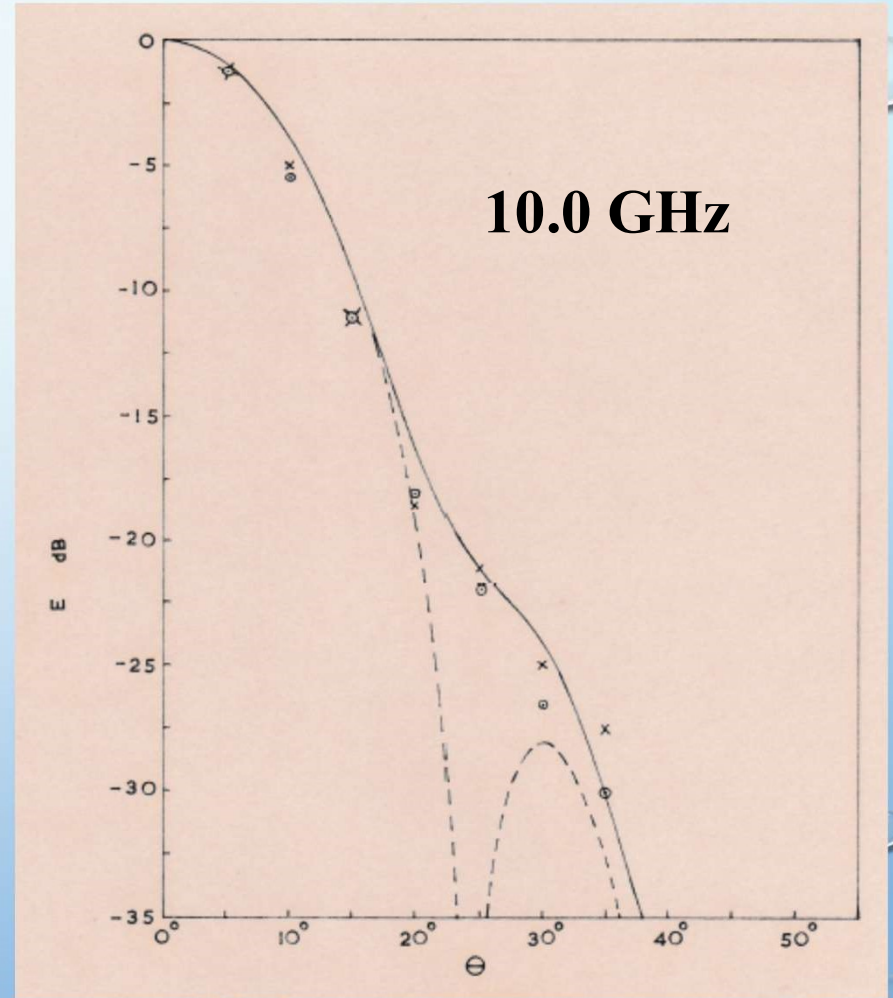
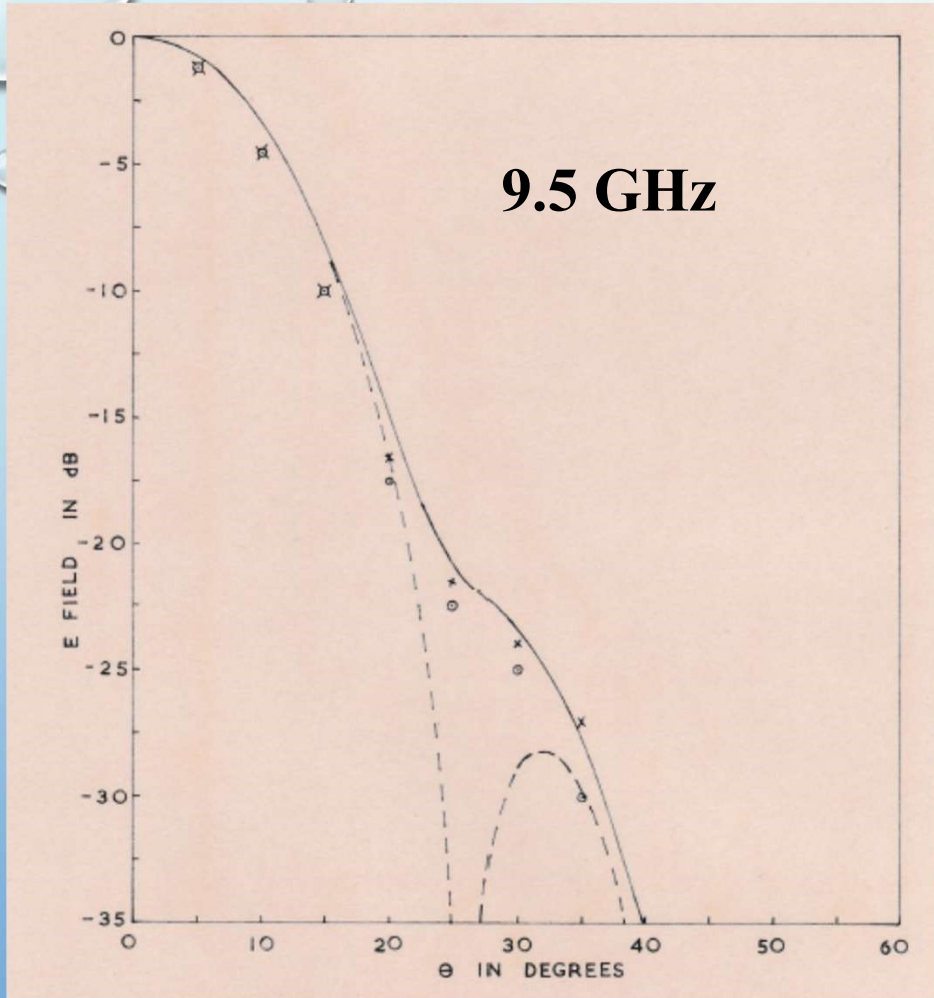
Narrow Flare Corrugated Conical Horn

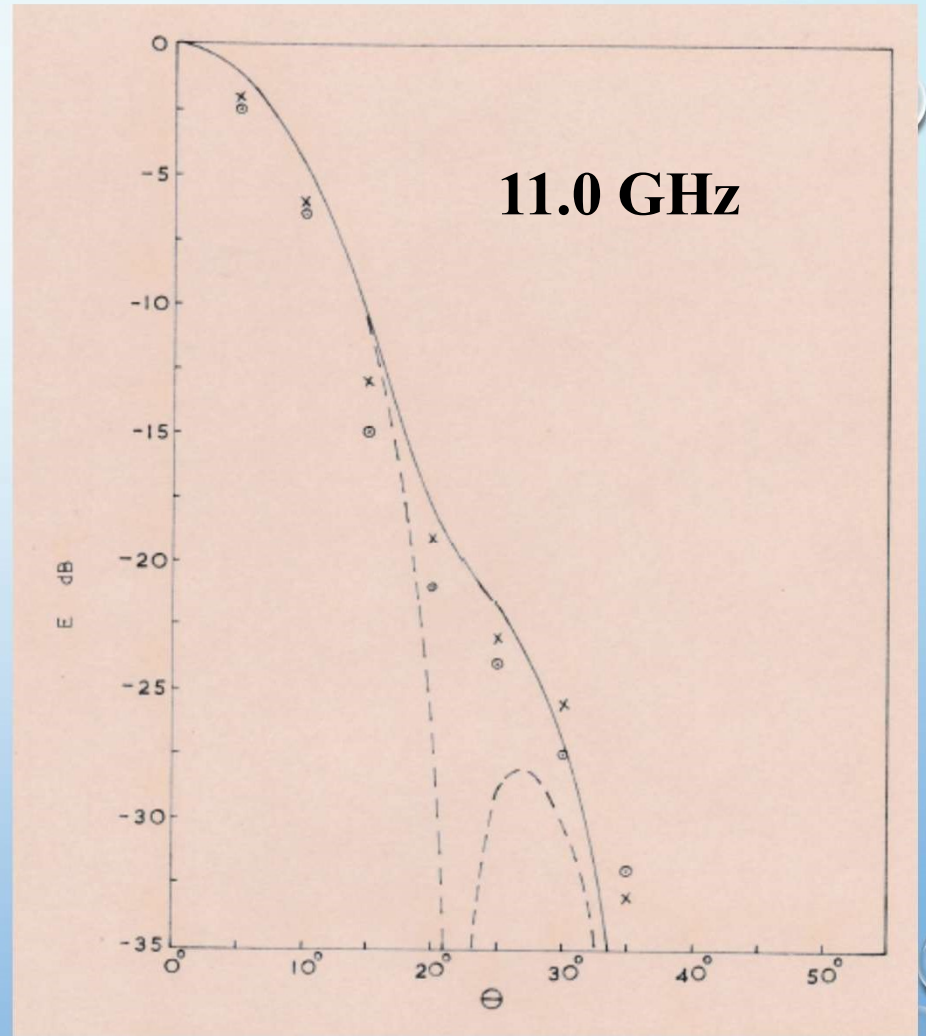
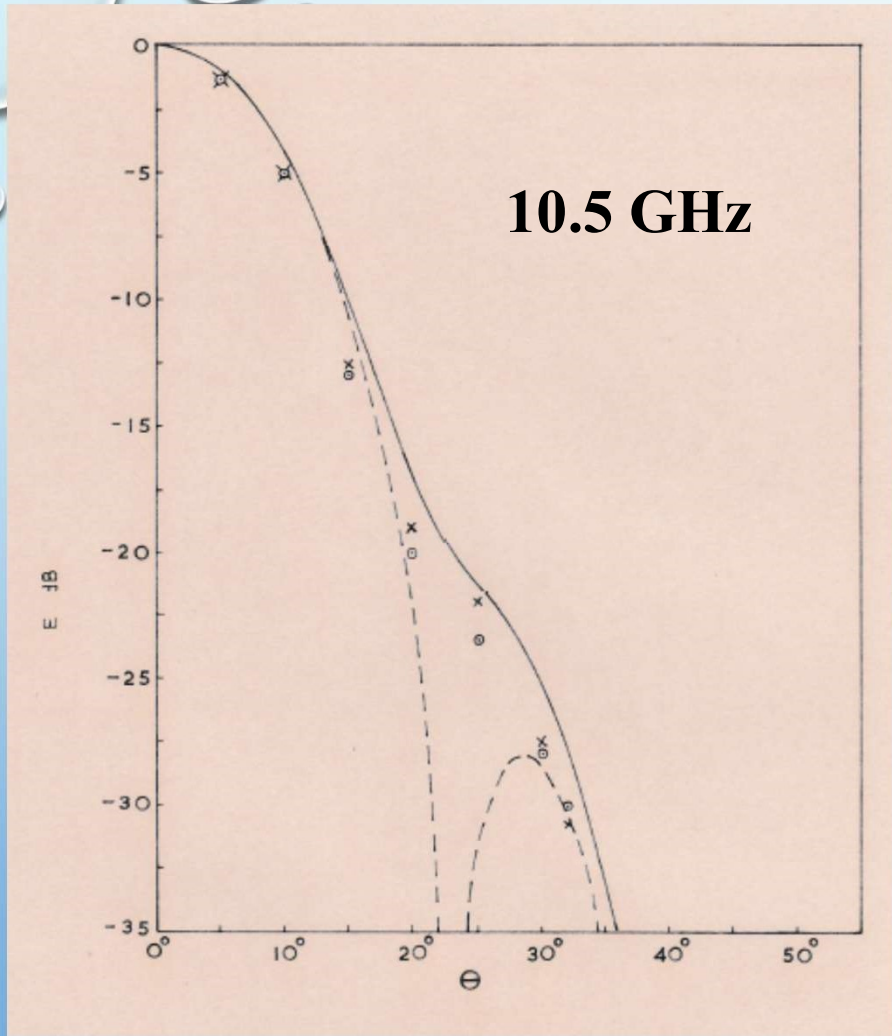


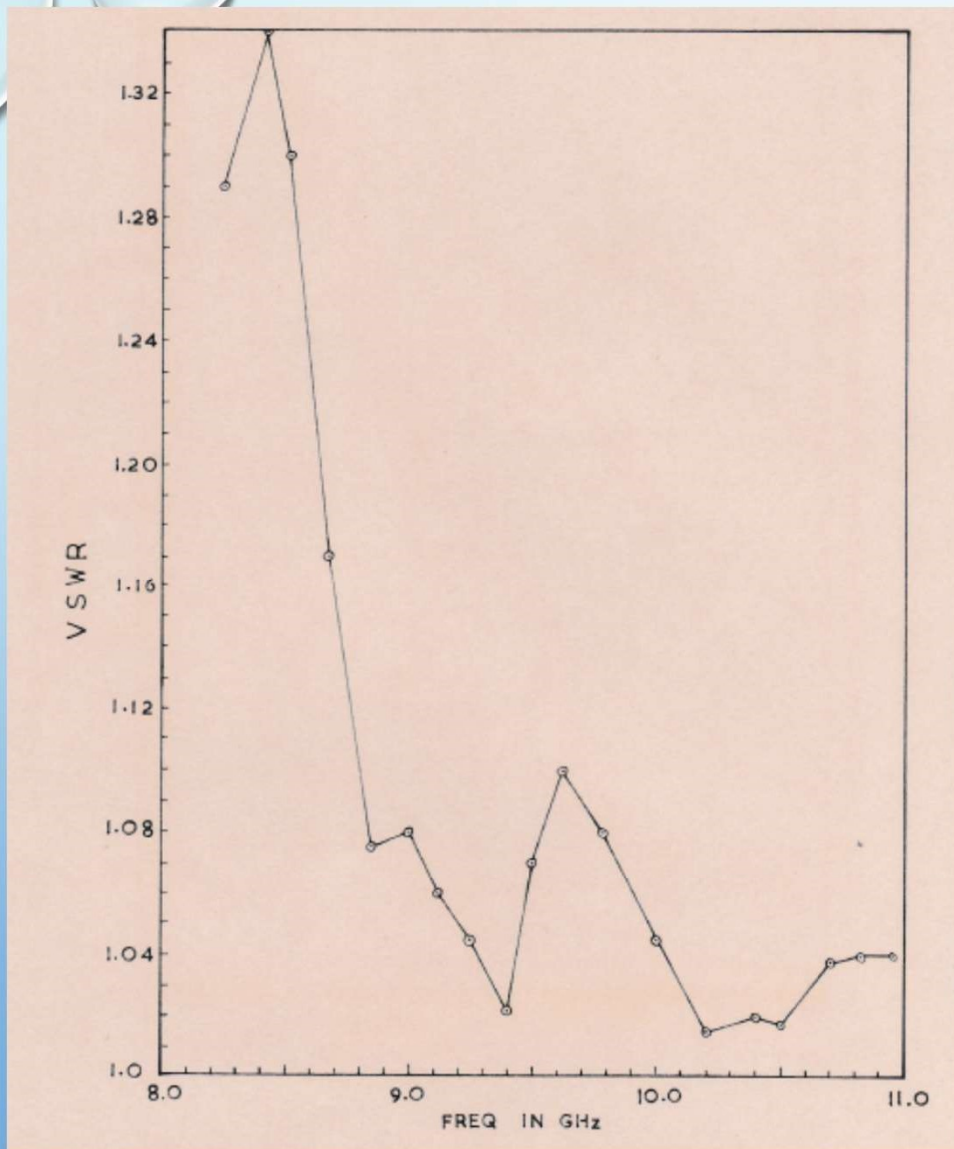
**Experimental X-Band 12° Half Flare
Corrugated Horn**

Theoretical and Measured Patterns of Experimental 12° Half Flare Horn

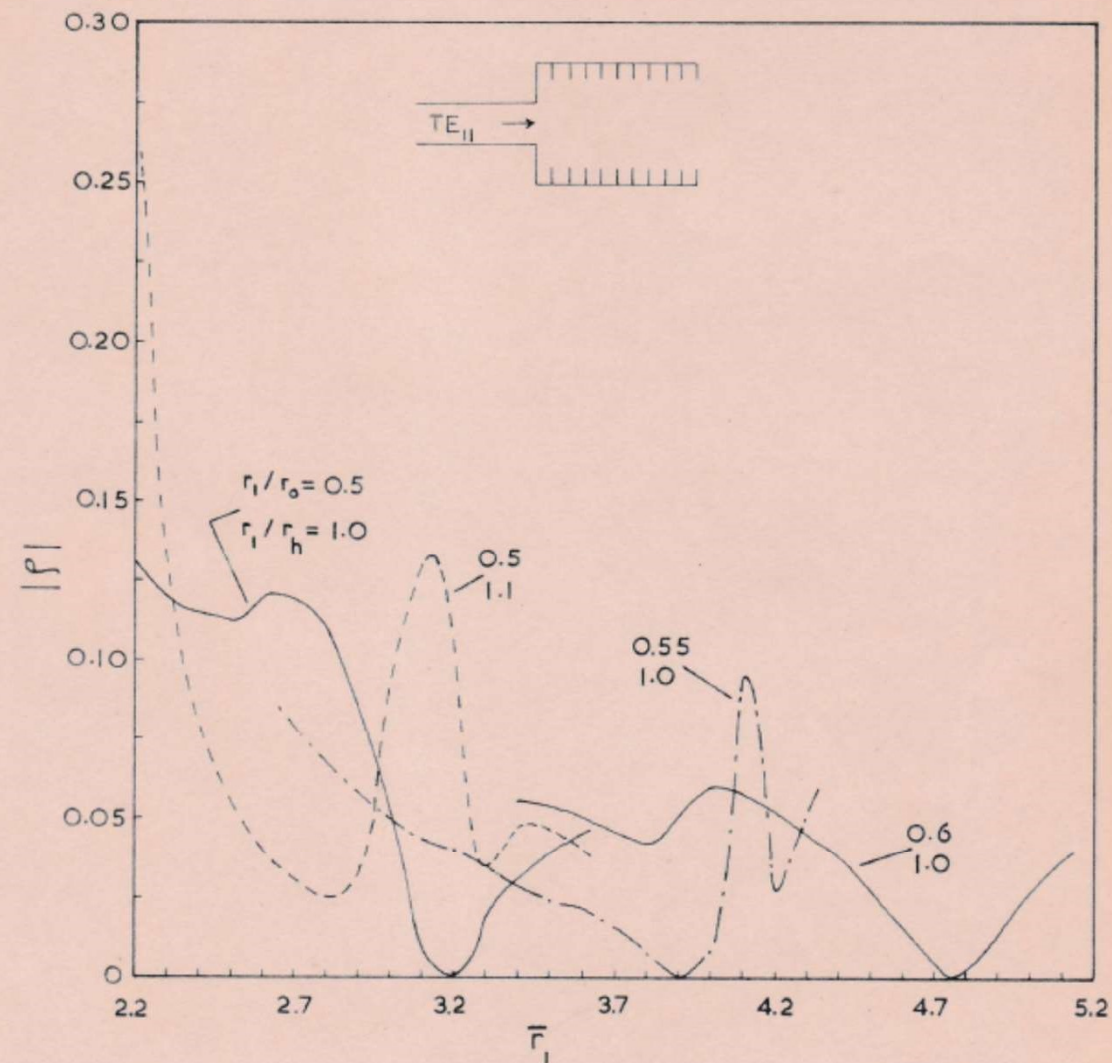








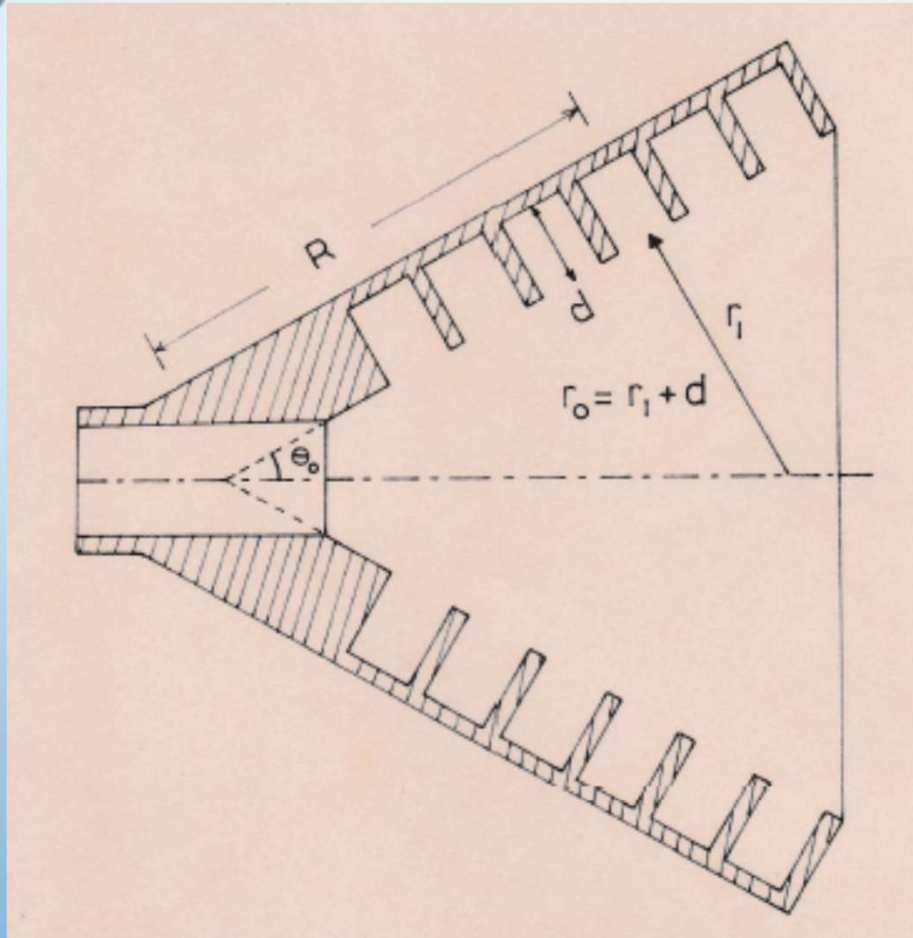
**Measured Input VSWR
at the throat of the
Experimental Narrow
Flare Horn of 12° Half
Flare Angle as Function
of Frequency**



Theoretically computed Reflection Coefficient at the junction of a TE_{11} circular waveguide and a corrugated circular waveguide as a function of normalized frequency for various waveguide parameters

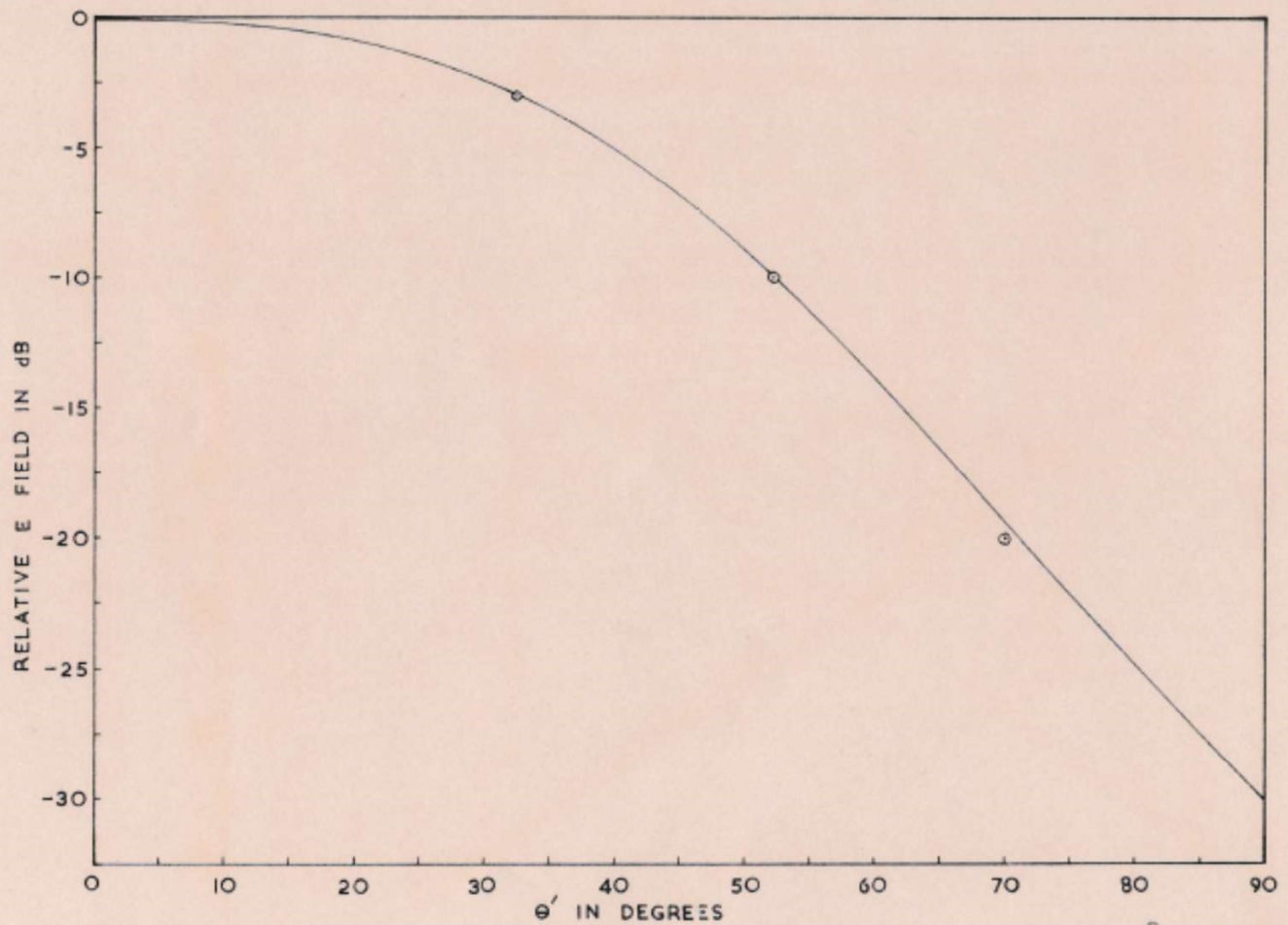
Propagation and Radiation Characteristics of Wide-flare Corrugated Conical Horn

- **Spherical Hybrid Modes in the Horn and Aperture Field**
- **Far-field pattern by vector diffraction**
- **Radiation Field by Spherical Wave Expansion**
- **Computation of Phase-Centre Location**
- **Lens-corrected Scalar Feed**
- **Performance of Parabolic Reflector with Scalar Feed**
- **An Experimental 30° Half-Flare Corrugated Conical Horn**
- **Experimental Results**
- **Modified Scalar Horn with Corrugations only near Aperture**

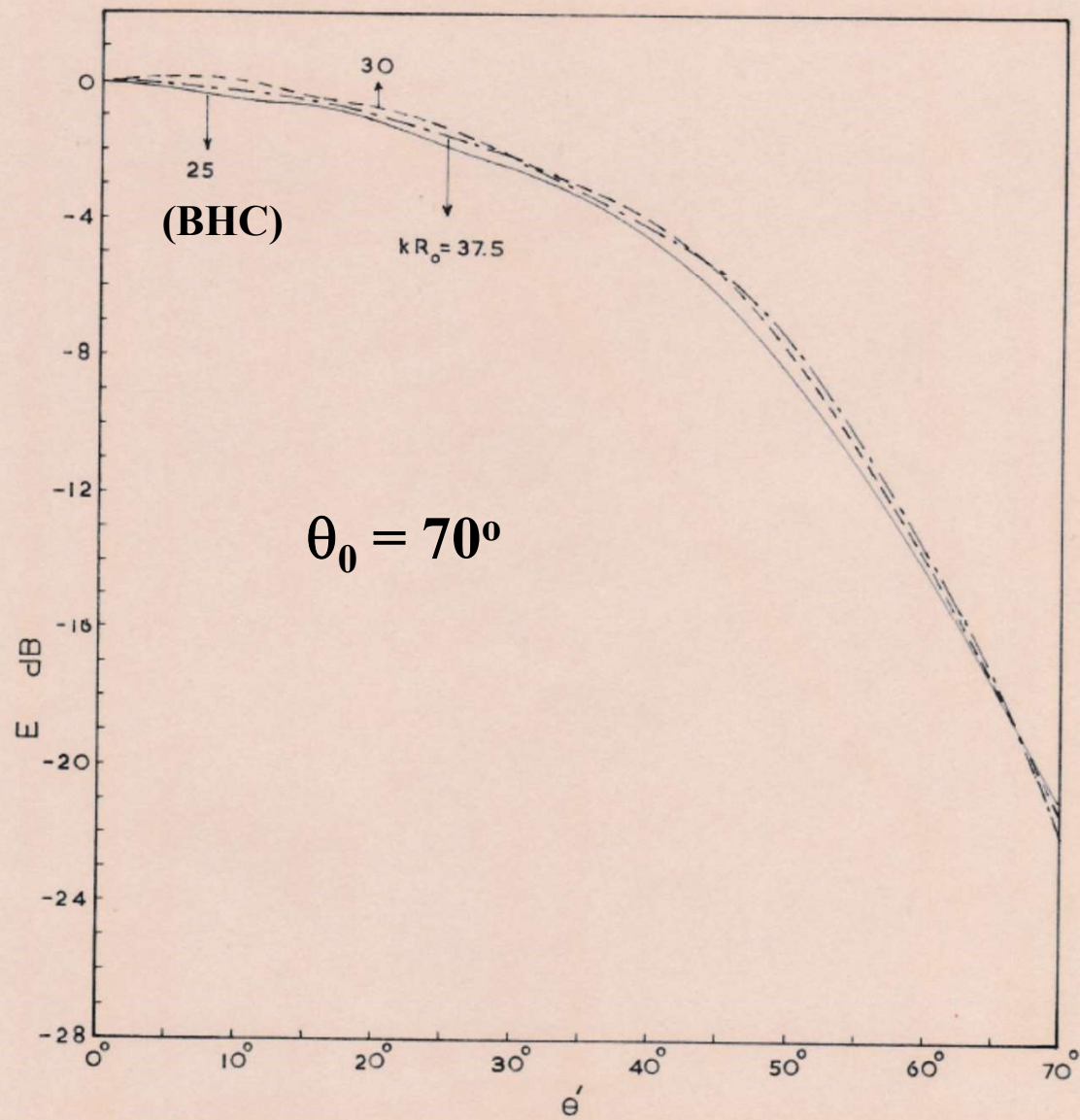


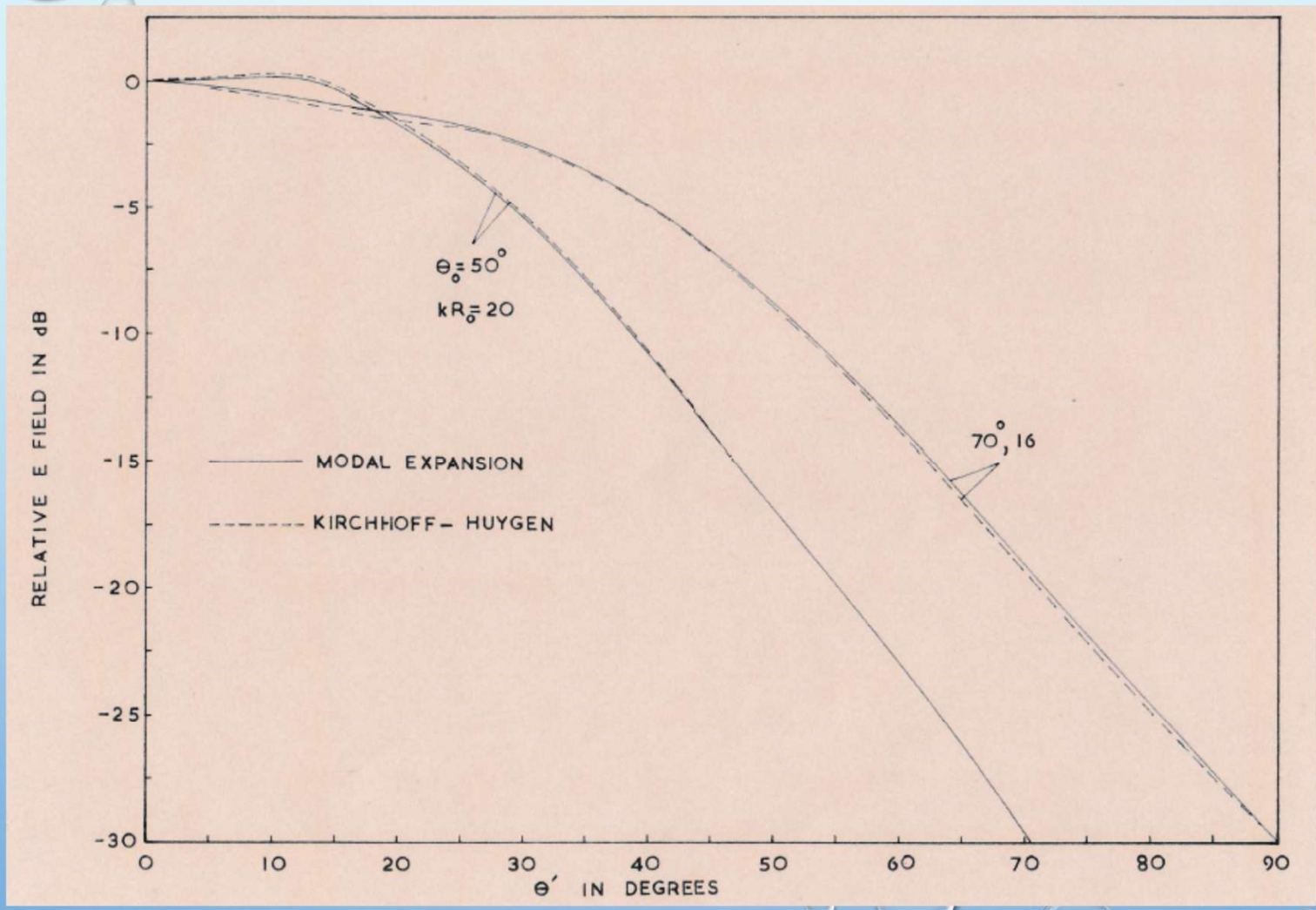
Wide Flare Corrugated Conical Horn

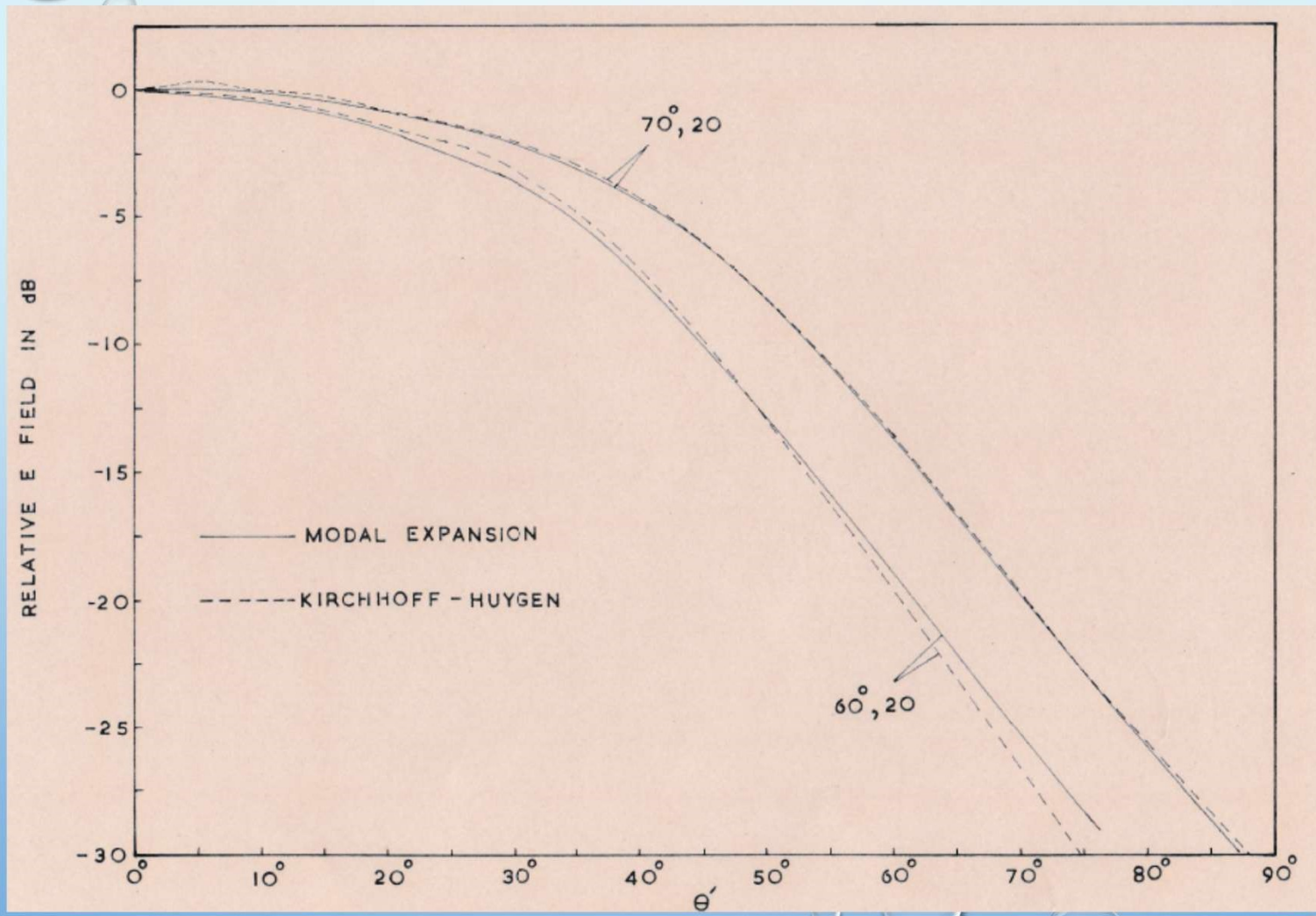
Impedance
boundary
condition
becomes
function of R .

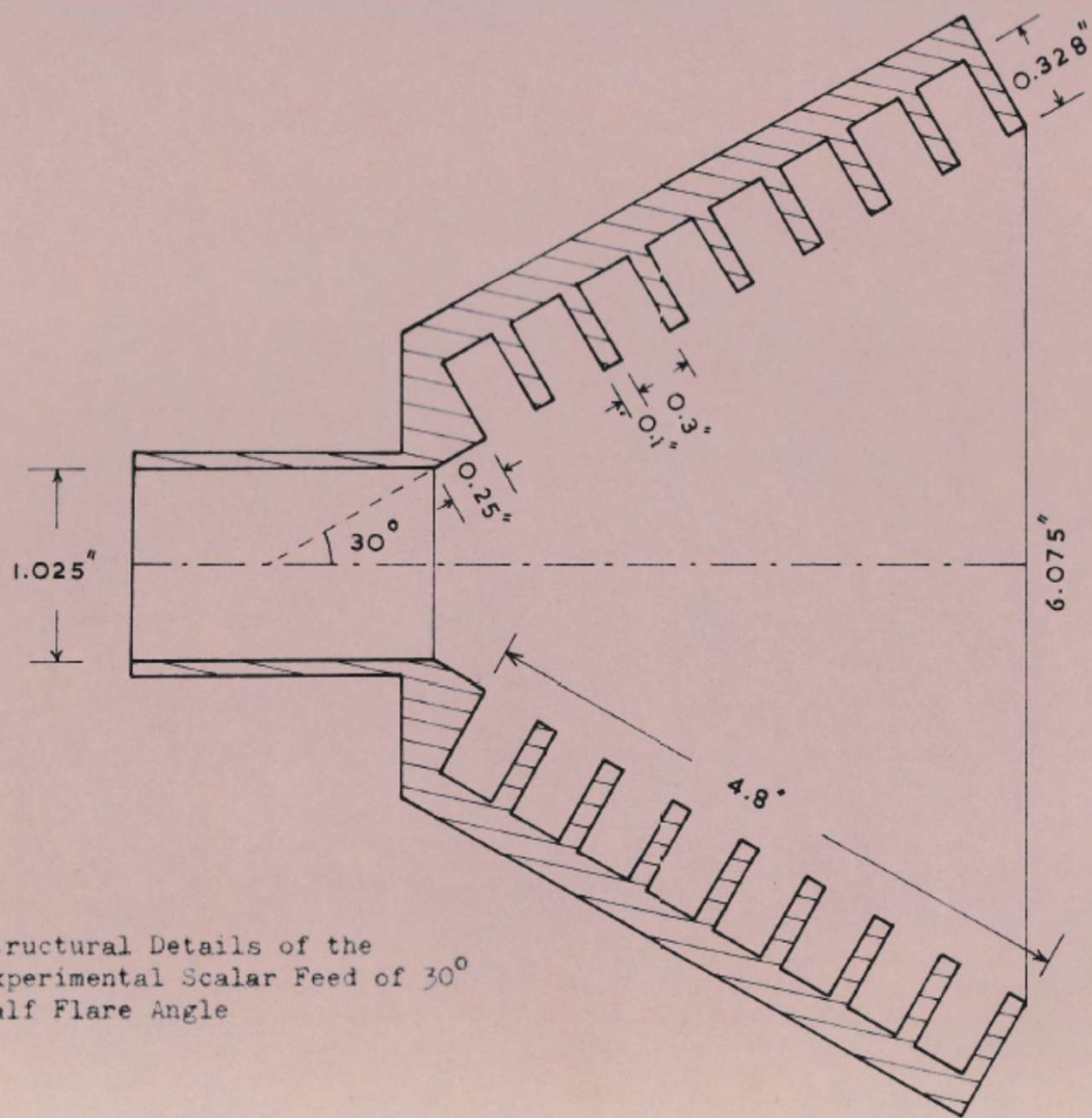


Theoretical Radiation Pattern of Corrugated Horn of 70° Half Flare Angle agrees almost exactly with experimental data of Kay's Scalar Horn



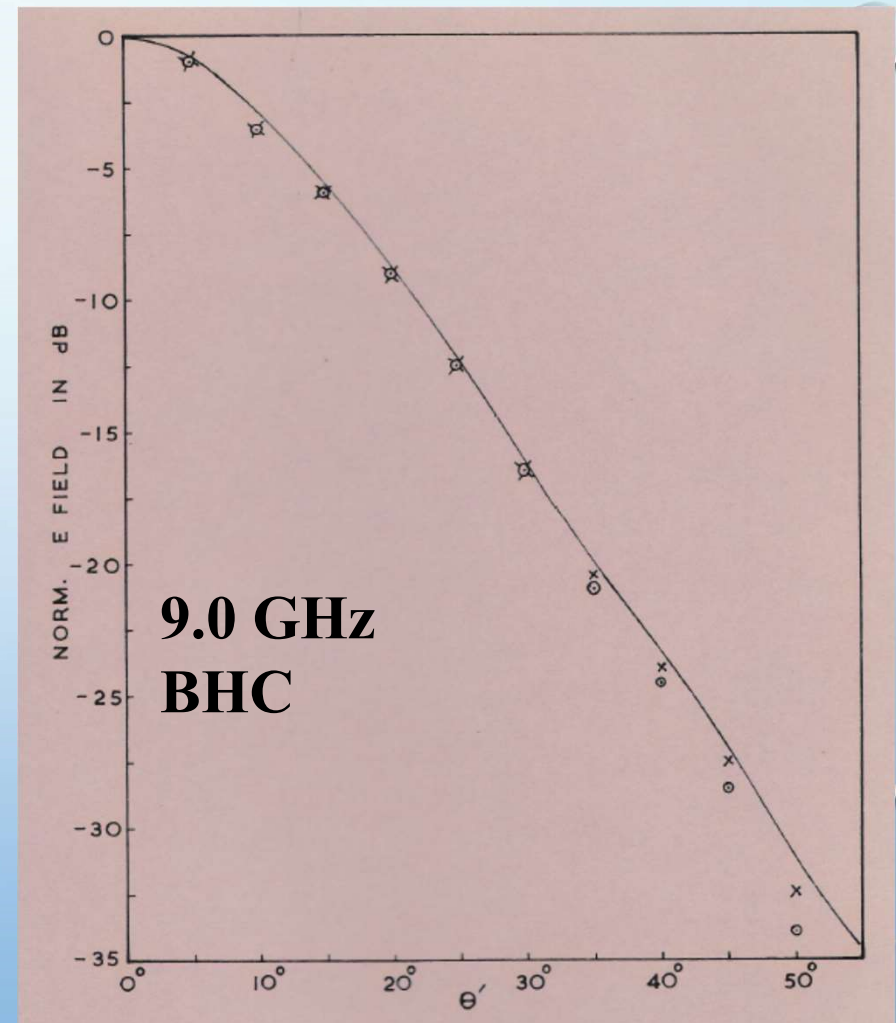
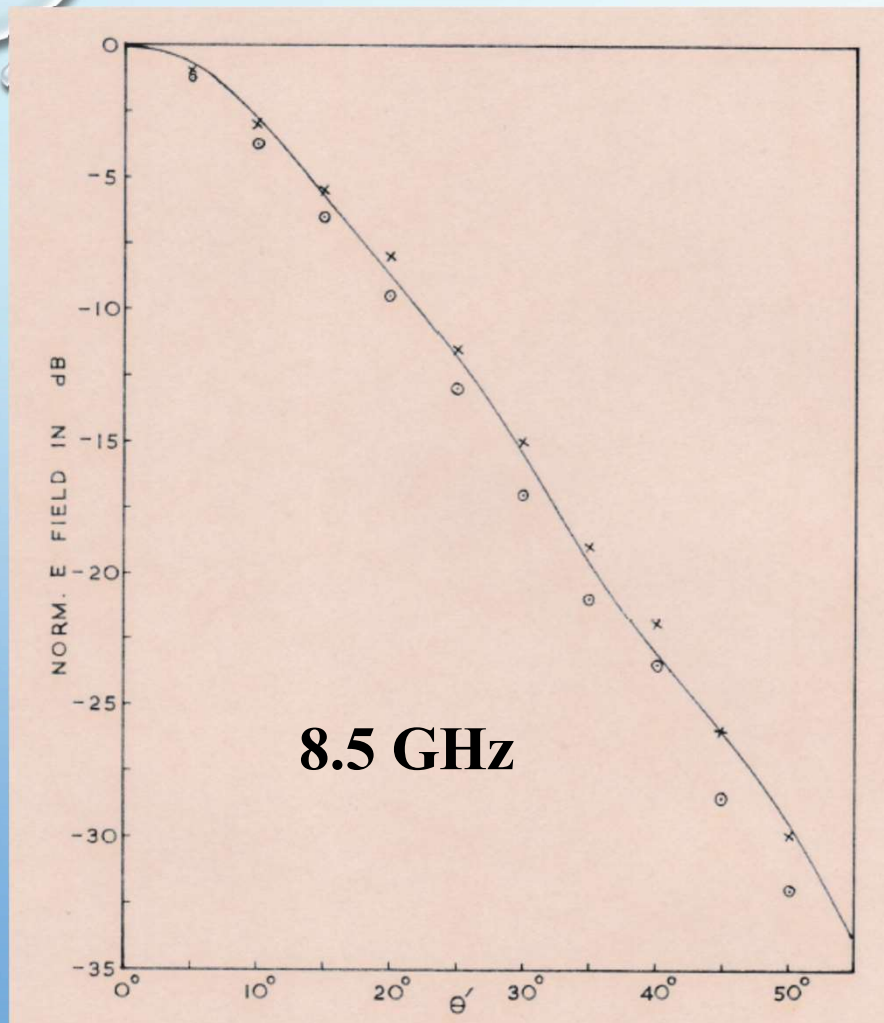


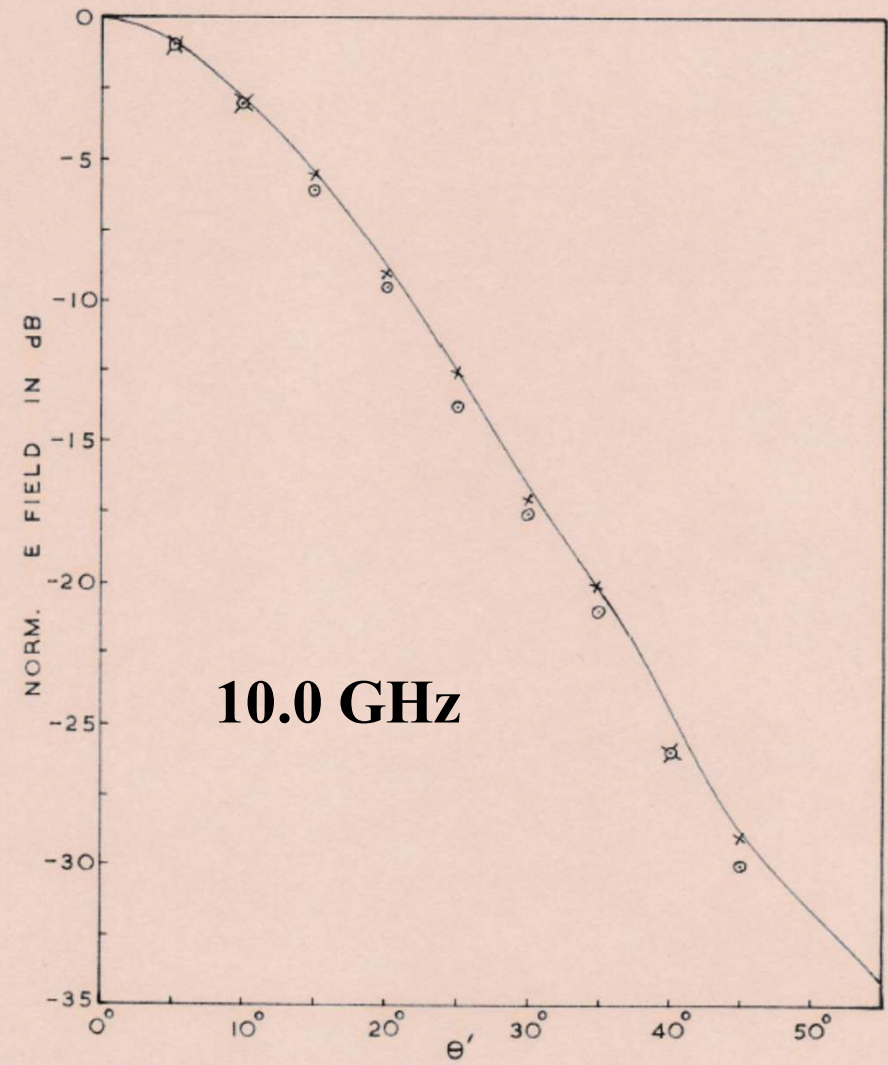
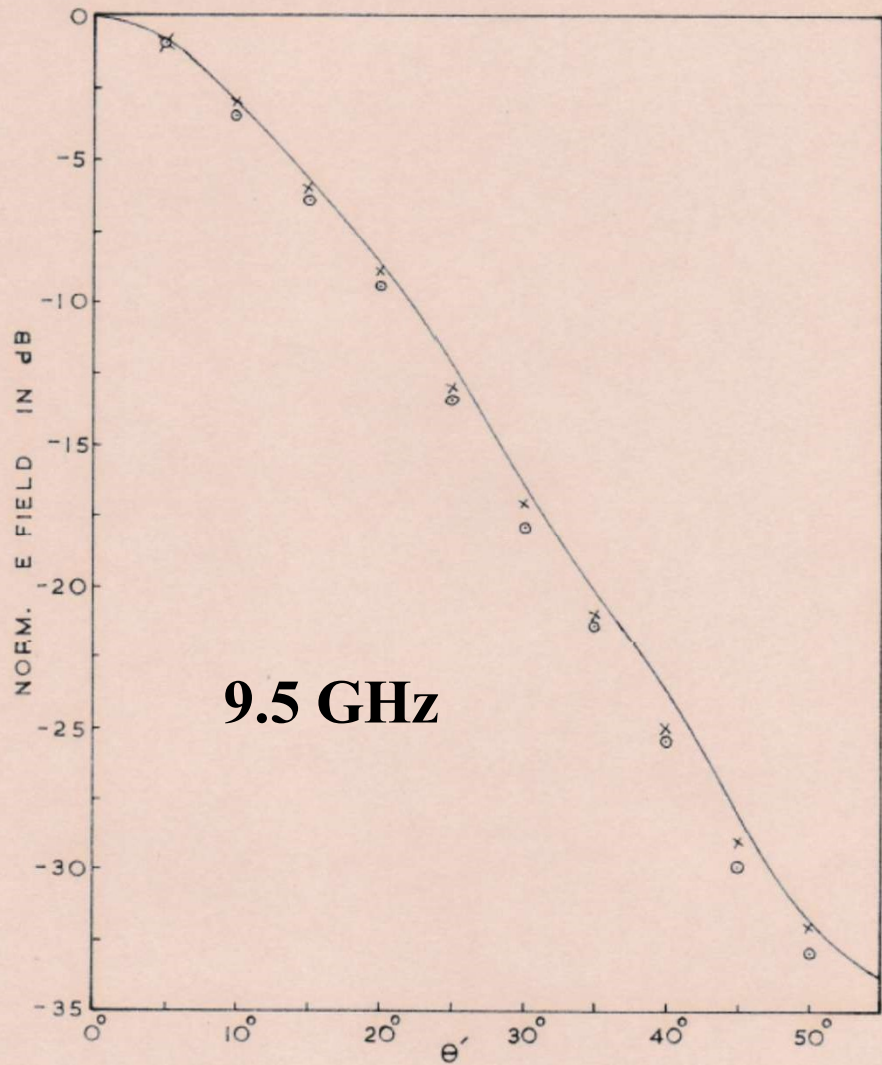


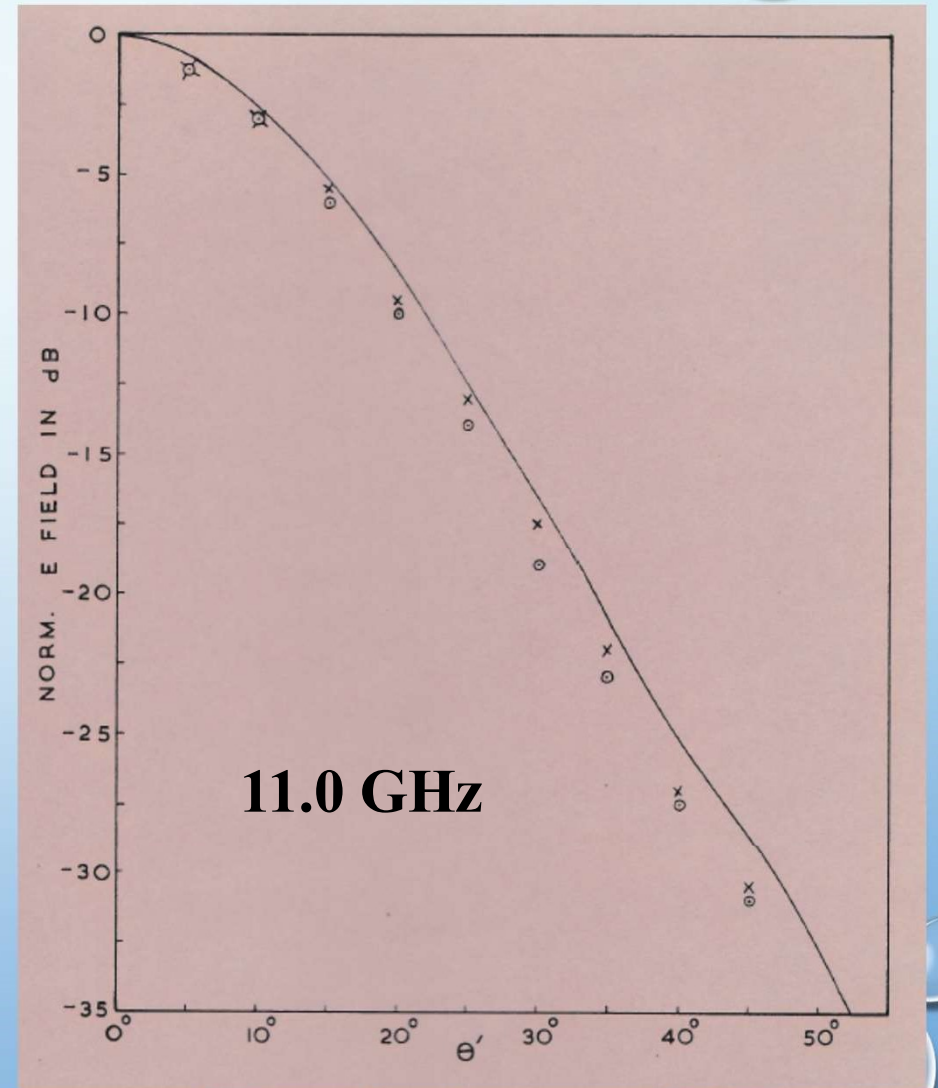
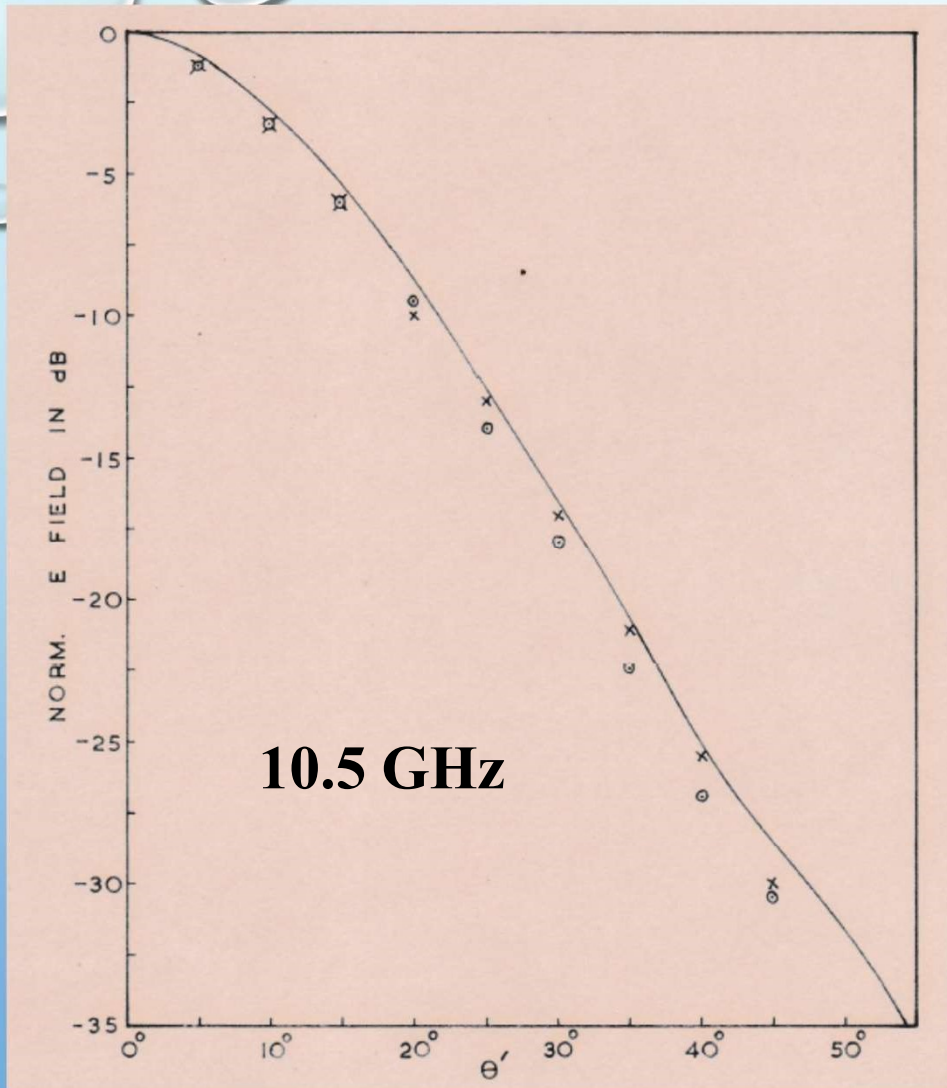


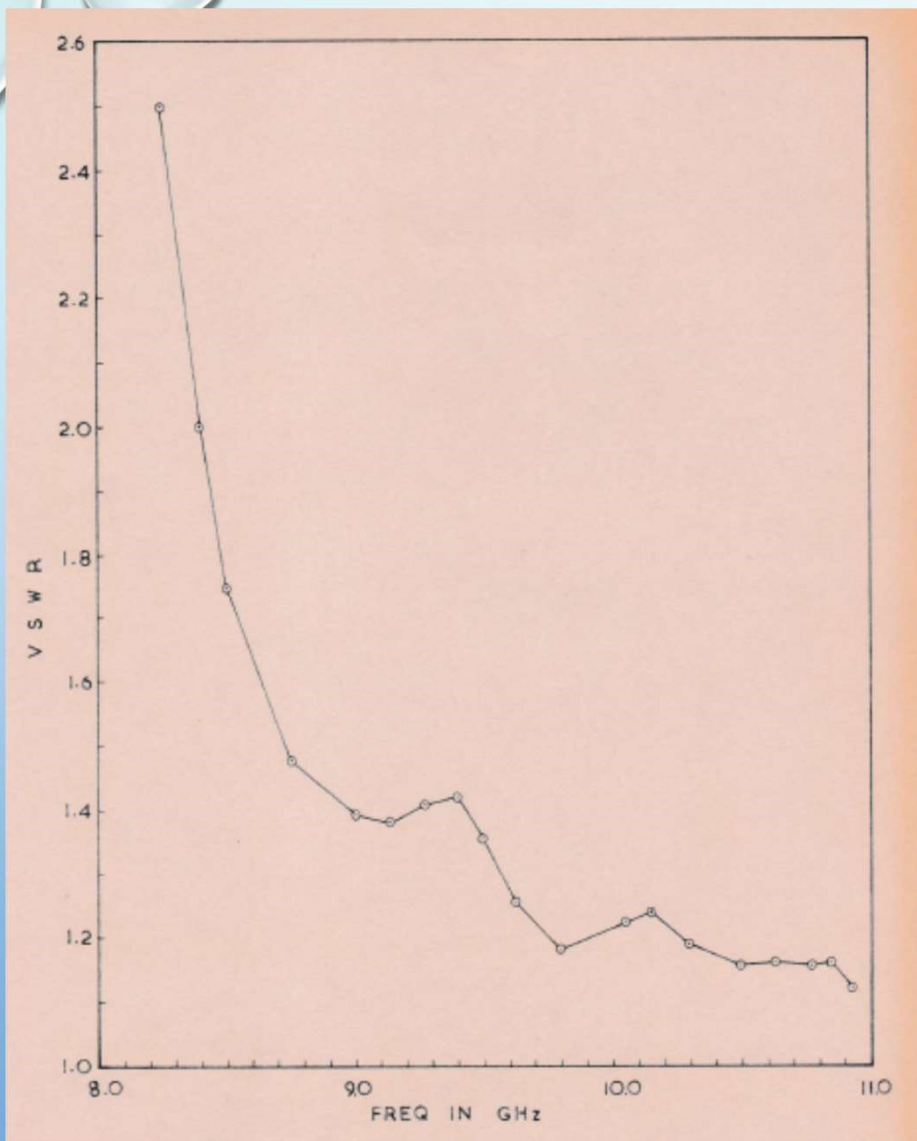
Structural Details of the Experimental Scalar Feed of 30° Half Flare Angle

Theoretical and Measured Patterns of Experimental 30° Half Flare Horn

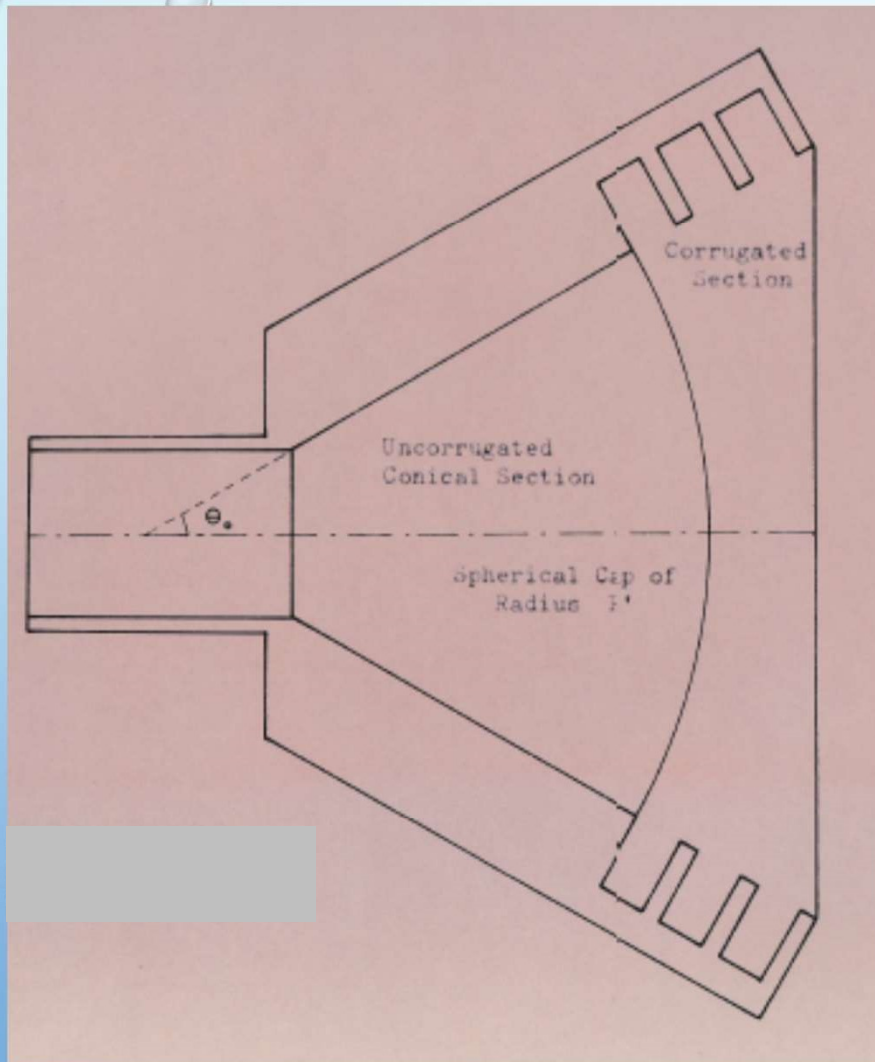








**Measured Input
VSWR at the throat
of the Experimental
Wide Flare Horn of
30° Half Flare Angle
as Function of
Frequency**



Modified Wide-Flare Corrugated Conical Horn with Corrugations only near the Aperture

**Excitation of Hybrid
Modes in Corrugated
section was computed by
mode matching over the
spherical cap at the
junction.**

Excitation of Modified Conical Scalar Horn

P_m/P_{in} in for first six modes

m	P_m/P_{in} in per cent				
	$\theta_o = 30^\circ$	$\theta_o = 40^\circ$	$\theta_o = 50^\circ$	$\theta_o = 60^\circ$	$\theta_o = 70^\circ$
1	83.87	83.36	82.67	81.79	80.67
2	4.39	4.56	4.80	5.11	5.53
3	3.59	3.69	3.81	3.96	4.13
4	1.36	1.40	1.46	1.54	1.64
5	1.27	1.31	1.35	1.41	1.49
6	0.68	0.70	0.73	0.76	0.81

Modified Scalar Feed: Observations from Computed results

- ❖ **Mode-matching equations were solved with 6 modes each in corrugated and un-corrugated sections for different flare angles.**
- ❖ **The reflection coefficient of the incident TE_{11} mode and excitation of higher order modes in un-corrugated section are negligible.**
- ❖ **The fraction of the incident power transferred to the modes in the corrugated section decreases sharply for the higher order modes and is less than 1% for the 6th mode.**

Thank You